

Fires from a cylindrical forest fuel burner : combustion dynamics and flame properties.

Dupuy J-L., Maréchal J., Portier D.

I.N.R.A. Unité de Recherches Forestières Méditerranéennes, Avignon, France

Morvan D.

Université de la Méditerranée, UNIMECA, Marseille, France

Keywords: forest fire behaviour, turbulent diffusion flame, flame height, temperature, gas velocity.

ABSTRACT: An experimental apparatus was designed to simulate and study, in laboratory conditions, the flame and the near-field plume stemming from the combustion of an isolated shrub that would be ignited by a surface fire. The main objective is to provide experimental data for the testing of a complete physical model of forest fire behaviour. The laboratory fire source (burner) was made of a cylindrical wire mesh basket filled with a forest fuel ignited at the lower circumference of the basket. A balance recorded the mass loss of the fuel sample and thus enabled to characterise the regime of combustion. Three diameters and two forest fuels were used to obtain different regimes. In addition, a specific device enabled to vary the air supply to the burner. In any case, the regime of combustion was non-steady over the whole duration of the test. Temperatures were measured using type K thermocouples of 50 μ diameter. 28 thermocouples were placed along the vertical axis of the device and along four horizontal lines. In addition, three pairs of thermocouples of which the signal was recorded at a high frequency (200 Hz), were used to determine the upward gas velocity at different heights along the vertical axis thanks to the cross-correlation of thermal fluctuations. Flame heights were obtained from the video recording of each test. The usual scaling laws that enable to relate flame height, temperature profiles and upward gas velocity profiles to steady burner characteristics in the upper part of the flame and in the plume, hold for the maximum flame height, for the maximum temperatures and (less clearly) for the maximum upward velocities observed with the present non-steady burner. But some of the parameters of these laws numerically differ from those obtained in earlier studies of turbulent diffusion flames.

1 INTRODUCTION

The physical modelling of forest fire behaviour is based on the resolution of a more or less complete system of conservation equations (mass, momentum, energy) that control the evolution of the coupled physical system formed by the vegetation and the surrounding gas mixture. Recently, a new generation of models is developed that tend to include more and more physical mechanisms (Grishin 1997, Linn 1997, Larini & al 1998, Margerit & Séro-Guillaume 2002). In particular, we are currently developing a forest fire spread model based on the multiphase approach firstly described by Larini & al (1998), which includes the main basic mechanisms of interest (Morvan & Dupuy 2001). At present, the conservation equations of the model are solved in a two-dimensional

vertical plane and can describe the propagation of a fire line in a real vegetation but still over a limited spatial domain (Morvan & *al* 2002a,b).

An essential feature of the development of such a model is to validate, and if necessary to improve, the numerous sub-models that describe the physics of the fire, namely the thermal degradation of the fuel (water vaporization, pyrolysis of dry material), the drag forces exerted by the fuel particles on the gas flow, the convective heat transfer between the fuel particles and the gas flow, the radiation in the fuel+gas mixture (burning zone) and gas+soot mixture (flames), the soot production and oxidation, the gas phase combustion of pyrolysis products, the combustion of chars, and also the turbulent effects on some of these processes. Up to now, the model predictions were mainly compared to fire experiments (laboratory or field) in terms of the predicted and observed rates of spread. An example is provided in Morvan & Dupuy (2001). In order to identify which mechanisms are well described by the model and which are not, it's necessary to focus on some features of the overall phenomenon and to take an interest in the physical properties of the medium.

That's the reason why we built an experimental device, which enables to study the properties of a flame stemming from the combustion of a forest fuel. The fire source was made of a cylindrical wire mesh basket filled with a forest fuel, which was ignited along the lower circumference of the basket. We chose this mode of ignition in order to roughly simulate the combustion of an isolated shrub that would be ignited by a surface fire. Hence, the physical system is expected to be axi-symmetric and has the advantage to be at rest in the horizontal plane, in contrast to propagating laboratory fires. This greatly facilitates the measurements and enables to determine the combustion regime (i.e. evolution of mass loss). The physical measurements were limited, in the present work, to temperature measurements with thermocouples. A video camera recorded the images of the fire in a vertical plane to determine flame geometry, in particular the flame height. Some of the thermocouples were used to estimate the upward velocity of gases at different heights using an analytical method based on the cross-correlation of thermal fluctuations (Cox 1977). Three basket diameters and two kinds of fuel were used and a special device enabled to change the air supply to the fuel. Combining these factors that are expected to change the combustion regime, 36 fires were realized (3 replications per treatment).

The present experimental results are compared with the conclusions of earlier studies of turbulent diffusion flames reviewed by Zukoski (1995) and Drysdale (1998).

An axi-symmetric solution of the two-dimensional model of fire behaviour to which we referred above, has been recently implemented and will be used in a future work to compare the predictions of the model to the present experimental results.

2 METHOD

2.1 *Experimental apparatus*

Fig. 1 shows a photograph of the apparatus. A wire mesh cylindrical basket of 20 cm height, devoted to contain the fuel, stands on an aluminium frame, which lays on a balance. A horizontal plate can be placed below the base of the basket (removable plate). Three baskets of 20, 28, and 40 cm diameter respectively, are available.

The balance has a precision of 1 g and its signal is recorded at a frequency of 1 Hz. 28 thermocouples are placed along the vertical axis of the device and along four horizontal levels. Their signal is recorded at a frequency of 1 Hz. In addition, three pairs of thermocouples are placed along the vertical axis, respectively 0.5, 1.5 and 2.5 m above the top of the basket. Their signal is recorded at a frequency of 200 Hz. Fig. 2 shows the detailed position of the sensors. Thermocouples are chromel-alumel thermocouples of 50 μ diameter and have a precision of 1°C. Separated experiments were conducted to estimate the characteristic response time of the thermocouples in flames. The characteristic response time is the characteristic time of an exponential response to an "instantaneous" increment of temperature. The principle was to suddenly insert a thermocouple in the flame at the vicinity of a control thermocouple recording the

signal over the whole time of the experiment. The results with such thin thermocouples are strongly variables in the flame medium, but the order of magnitude of the characteristic response time was 0.1 s.

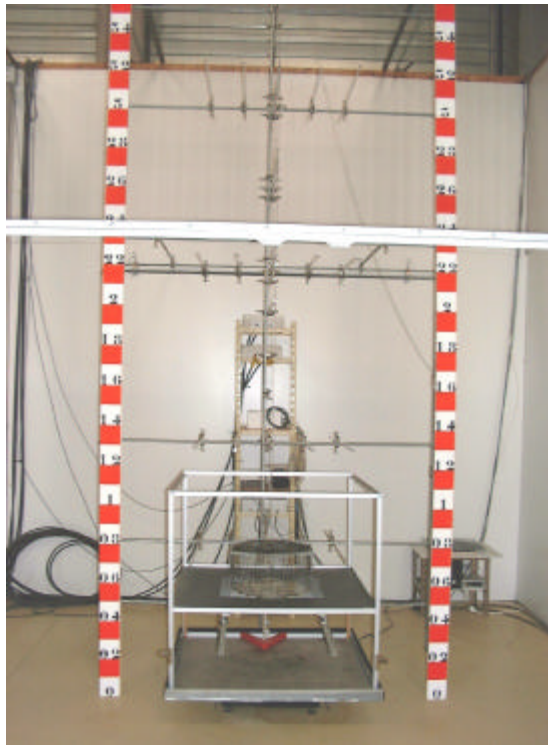


Figure 1. View of the experimental apparatus.

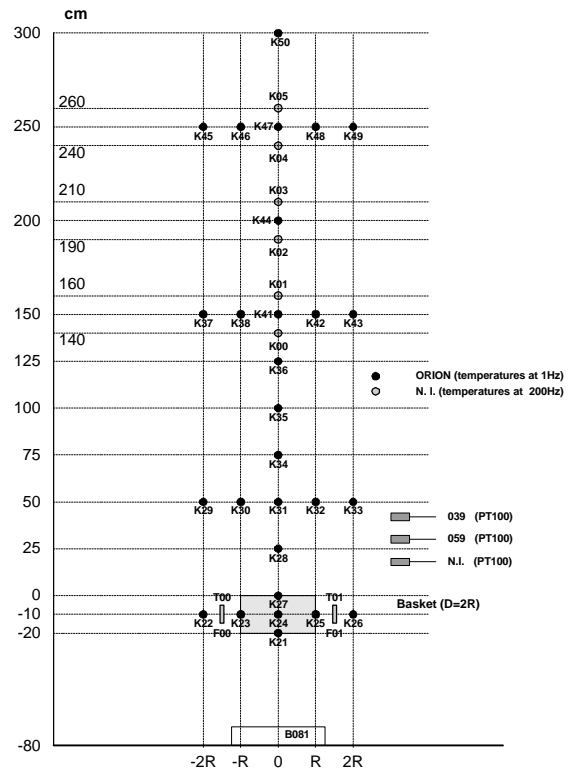


Figure 2. Position of the sensors.

2.2 Fuel and Ignition

The basket is filled with an oven-dried fuel as homogeneously as possible. Two kinds of fuel were used, *Pinus Pinaster* needles (PP) and excelsior (Exc). The amount of fuel (dry material) was adjusted to the size of the baskets so that the bulk density was constant for a given fuel (20 kg/m³ for PP, 8 kg/m³ for Exc). Hence, for baskets of 20, 28, and 40 cm diameter, the initial mass of fuel were respectively 125, 250 and 500 g for PP fuel and 50, 100 and 200 g for Exc fuel. The surface to volume ratio and density of PP particles were 4100 m⁻¹ and 640 kg/m³ respectively. The surface to volume ratio and density of Exc particles were 22000 m⁻¹ and 830 kg/m³ respectively.

A circular device of diameter equal to the basket diameter was designed to ignite the fuel using alcohol at the lower circumference of the basket. Hence, the combustion of the solid fuel spreads from the circumference to the centre of the basket.

The combination of the three basket diameters, of the presence or absence of the removable plate and of the two kinds of fuel, led to 12 different treatments. Each was replicated at least three times.

3 RESULTS

3.1 Combustion regimes

The mass loss rate of the fuel as a function of time is deduced from the recordings of the balance signal for each test. During the tests, a steady-state combustion regime was never achieved, as

illustrated in Fig. 3. A mathematical model describing the time evolution of the mass loss rate was fitted to the mass loss data for each test (e.g Fig. 3):

$$v = v_{\max} \left(\frac{t}{t_{\max}} \right)^a \exp \left(-a \left(\frac{t - t_{\max}}{t_{\max}} \right) \right), t \geq 0 \quad (1)$$

where v_{\max} is the maximum mass loss rate and t_{\max} the time at which this maximum is reached. The integral of equation (1) over $[0, +\infty)$ is a known value (initial mass of fuel, m_0). Thus, the parameters of equation (1) are not independent parameters and it can be shown that :

$$v_{\max} = m_0 \frac{a^{(a+1)} e^{-a}}{\Gamma(a+1) t_{\max}} \quad (2)$$

(Γ is the gamma function).

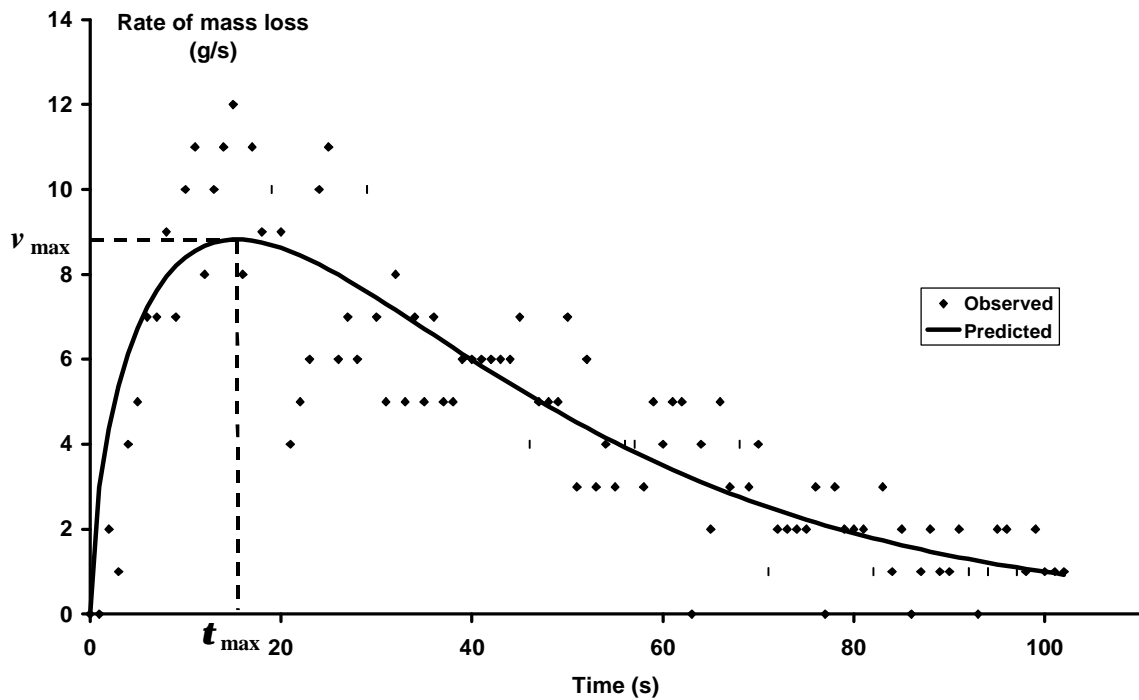


Figure 3. Time evolution of the rate of mass loss (Fuel=PP, $D=0.4$ m, Plate=Yes).

Fig. 4 illustrates the effect of the fuel type on the combustion regime (fitted curves). The fuel type does not affect the maximum mass loss rate (v_{\max}), but it clearly affects the characteristic time of the combustion regime (t_{\max}), which is lower for Exc fuel than for PP fuel. Fig. 5 shows the effect of the basket diameter on the combustion regime. The diameter mainly affects the maximum mass loss rate.

A statistical analysis of the estimated parameters of the model confirmed these results. In addition, it was found that the presence or the absence of the removable plate, has no effect on the combustion regime, except in the case of PP type combined with the larger diameter (40 cm). In this latter case, some puffing phenomena were observed at the end of the flaming combustion period, indicating that oxygen was probably missing inside the basket.

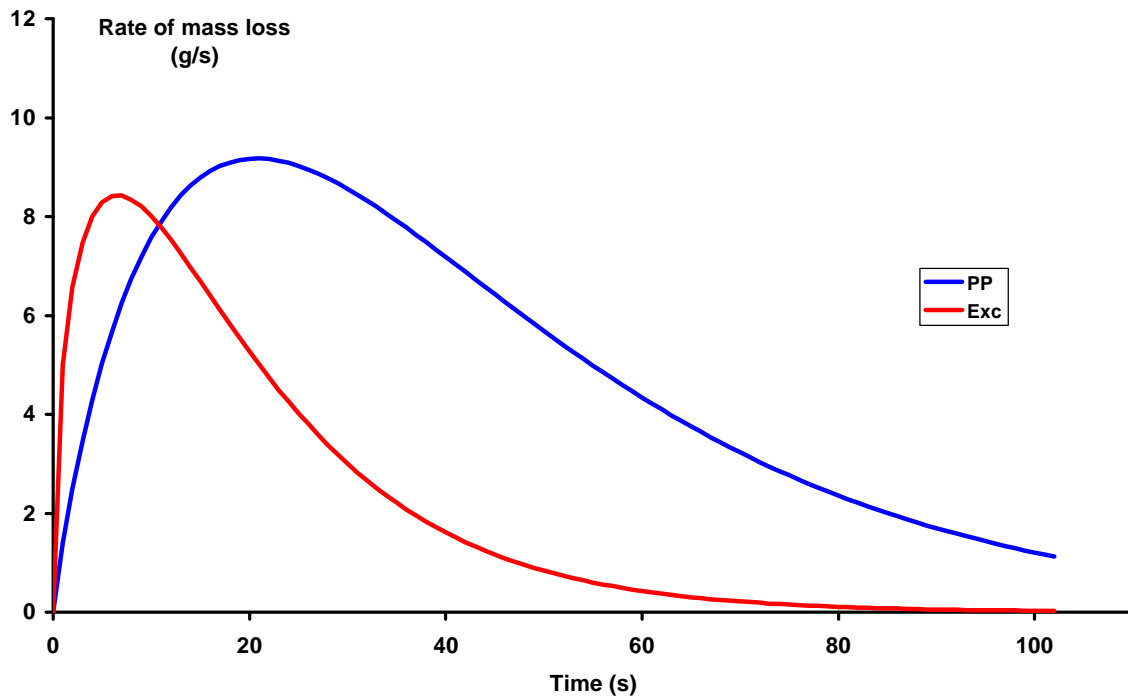


Figure 4. Effect of fuel type on the rate of mass loss ($D=0.4$ m, Plate=Yes).

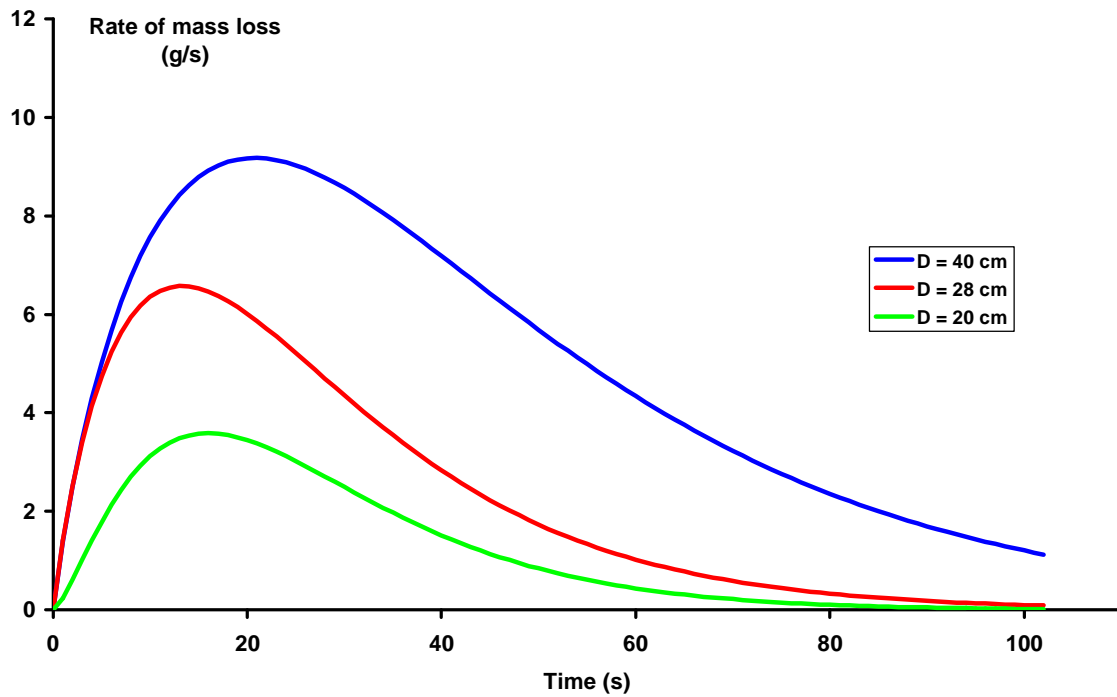


Figure 5. Effect of the burner diameter on the rate of mass loss (Fuel=PP, Plate=Yes).

The maximum heat release rate Q_{fmax} was calculated from the maximum mass loss rate estimated for each fire, using a heat of combustion of 18 kJ/kg. It ranges between 40 and 200 kW. The mean values of Q_{fmax} and t_{max} and their standard errors for each treatment are reported in Table 1.

Table1. Maximum values of the heat release rate ($Q_{f \max}$)

Basket diameter (cm)	Fuel	Plate ⁽¹⁾	$Q_{f \max}$ (kW)		t_{\max} (s)	
			mean	std err.	mean	std err.
40	PP	Yes	165	5	21	0.4
40	Exc	Yes	152	13	7	0.4
40	PP	No	189	5	18	0.3
40	Exc	No	173	7	7	0.2
28	PP	Yes	118	5	13	0.4
28	Exc	Yes	85	14	5	0.6
28	PP	No	113	3	18	0.3
28	Exc	No	98	7	7	0.3
20	PP	Yes	65	4	16	0.6
20	Exc	Yes	41	6	7	0.7
20	PP	No	60	2	15	0.4
20	Exc	No	45	4	9	0.5

(1) Horizontal removable plate located at the base of the basket (present : yes, absent : no)

(2) Time when the maximum heat release rate is achieved

3.2 Flame height

The flame height was measured using the video camera movies. The values were sampling every second. Fig. 6 shows an example of the time evolution of the flame height and of the corresponding mass loss rate. The maximum value of flame height is reached a few seconds after the maximum mass loss rate and it remains steady for about 20 s. Hence, despite a non-steady combustion regime, a period of quasi-steady and fully-developed flame is observed. The duration of this period depends on the combustion regime and ranged between 5 and 30 s.

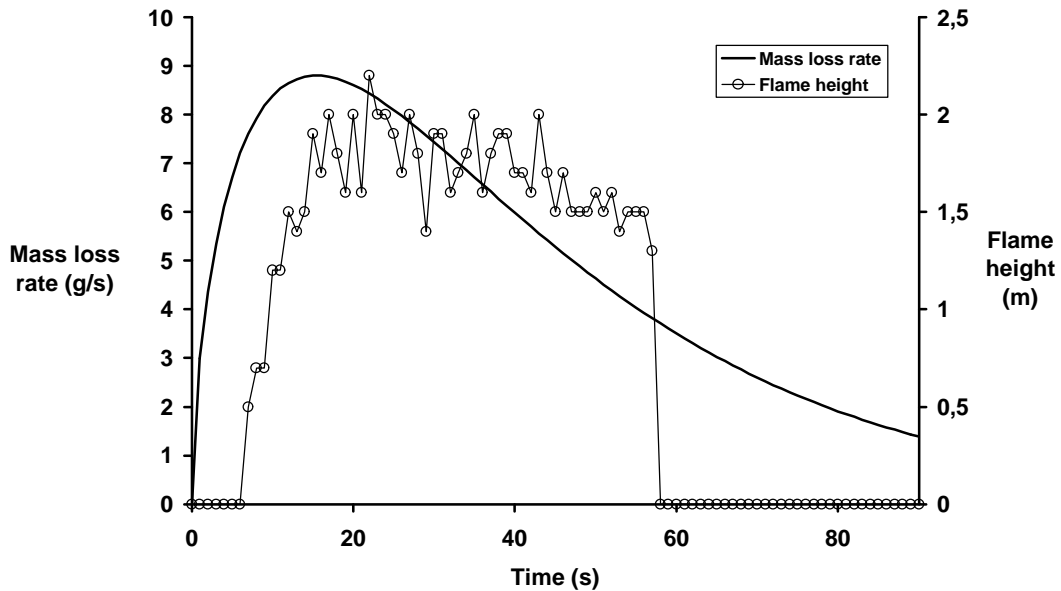


Figure 6. Comparative time evolutions of the rate of mass loss and of the flame height (Fuel=PP, $D=0.4$ m, Plate=Yes).

The maximum values of flame height H_{fl} were determined for each test. This value is defined as the maximum of a moving average calculated over the whole time evolution of height on a five second period.

The analysis of the maximum flame height variations with burner characteristics shows that the maximum flame height depends only on the maximum heat release rate. In particular, it does not depend on the burner diameter D and on the characteristic time t_{max} . Fig. 7 shows the maximum flame height H_{flmax} as a function of the maximum heat release rate Q_{flmax} . A simple power law well describes this function :

$$H_{flmax} = k Q_{flmax}^b \quad (3)$$

The estimated parameters are (mean, standard error) : $k=0.21$ (0.02), $b=0.43$ (0.02), with H_{flmax} (m), Q_{flmax} (kW).

Earlier theoretical and experimental studies of turbulent diffusion flames from porous gas burners have provided scaling laws for flame height and other important properties of the flame and the plume (Steward 1970, McCaffrey 1979, Zukoski & al 1981). The laws derived from these *steady* combustion regimes showed that the flame height scales as a $2/5$ power of the heat release rate for axi-symmetric fires :

$$H_{fl} = 0.2 Q_f^{2/5} \quad (4)$$

The parameters that we obtain on *non-steady* combustion regimes are not significantly different from the above ones. Hence, we define the characteristic flame height Z_{fl} as the value predicted by the equation (4).

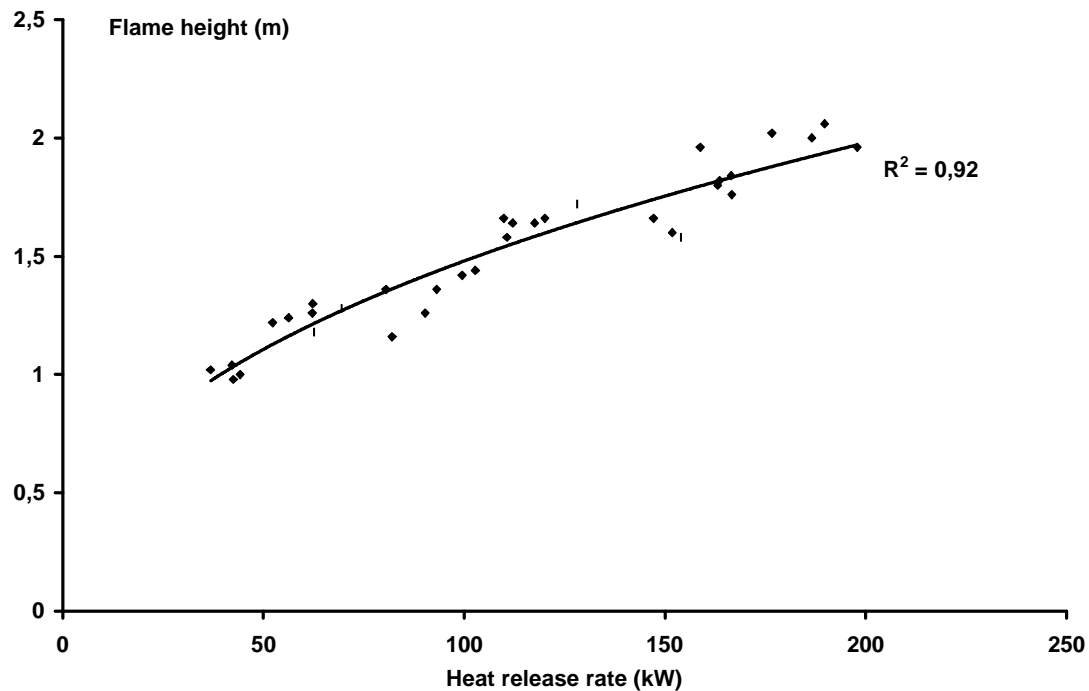


Figure 7. Maximum flame height *versus* maximum heat release rate.

3.3 Vertical temperature profile

Fig. 8 shows the time evolution of the centreline (vertical axis z) temperature at several heights above the burner.

The maximum values of the excess temperature ($T - T_a$) were determined for each test and for each measurement position. This value is defined as the maximum of a moving average calculated over the whole recording of temperature on a five second period.

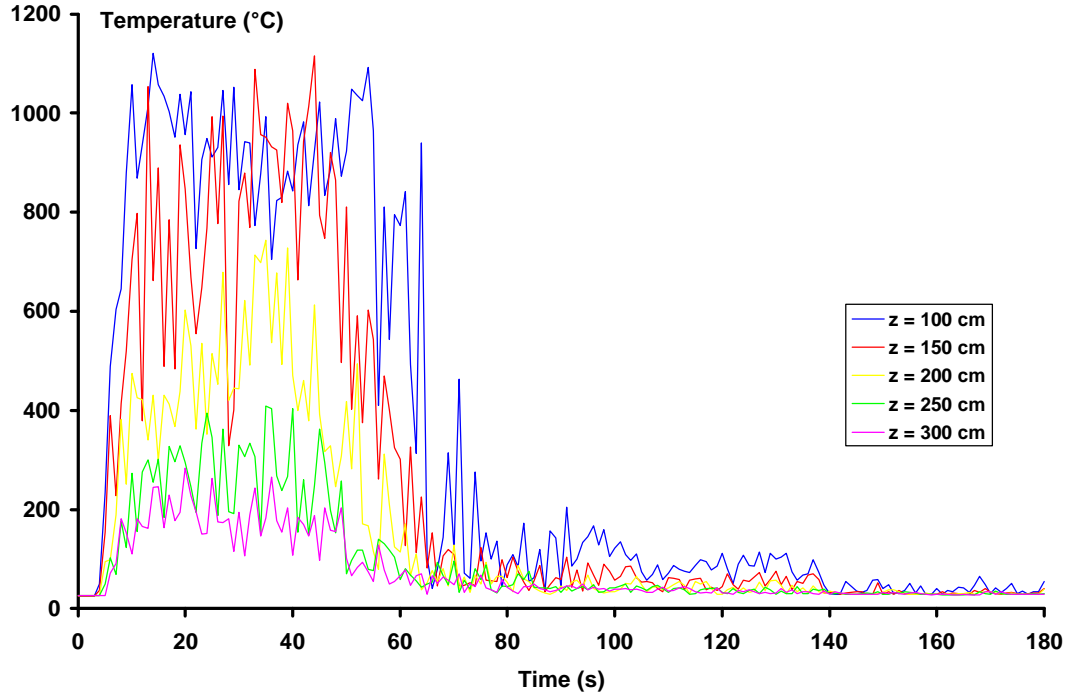


Figure 8. Time evolution of 1 Hz recorded temperatures at different vertical levels (Fuel=PP, $D=0.4$ m, Plate=Yes).

The maximum excess temperatures along the centreline ($T_m - T_a$), are well described when they are plotted versus the normalised height Z , defined as :

$$Z = \frac{z}{Z_n} \quad (5)$$

Fig. 9 shows this plot in logarithmic scales. The following model was fitted to the data for $Z > 0.3$:

$$\begin{aligned} \text{if } Z < Z_0 : \quad T_m - T_a &= T_0 - T_a \\ \text{if } Z_0 \leq Z < Z_1 : T_m - T_a &= (T_0 - T_a) \left(\frac{Z}{Z_0} \right)^{-b} \\ \text{if } Z_1 \leq Z : \quad T_m - T_a &= (T_0 - T_a) \left(\frac{Z_1}{Z_0} \right)^{-b} \left(\frac{Z}{Z_1} \right)^{-c} \end{aligned} \quad (6)$$

The estimated parameters are (mean, standard error) : $T_0 - T_a = 973$ (6) $^{\circ}\text{C}$, $Z_0=0.75$ (0.02), $Z_1=0.97$ (0.02), $b=0.86$ (0.12), $c=2.17$ (0.06).

The model is similar to that obtained by McCaffrey (1979) from a gas porous burner (methane, $D=0.3$ m), but some of the estimated parameters differ between the two studies. McCaffrey reported $T_0 - T_a = 800^{\circ}\text{C}$, $Z_0=0.4$, $Z_1=1$, $b=1$, $c=5/3$, and the model applied for $Z > 0.15$.

We notice that $Z=0.75$ roughly corresponds to the beginning of the intermittent region of the flame and $Z=1$ corresponds to the average flame height center of the intermittent region. Values observed for $Z < 0.3$ cannot be described by such a simple model. They are related to the influence of the diameter and combustion regime on the flow shape just above the basket (flame base).

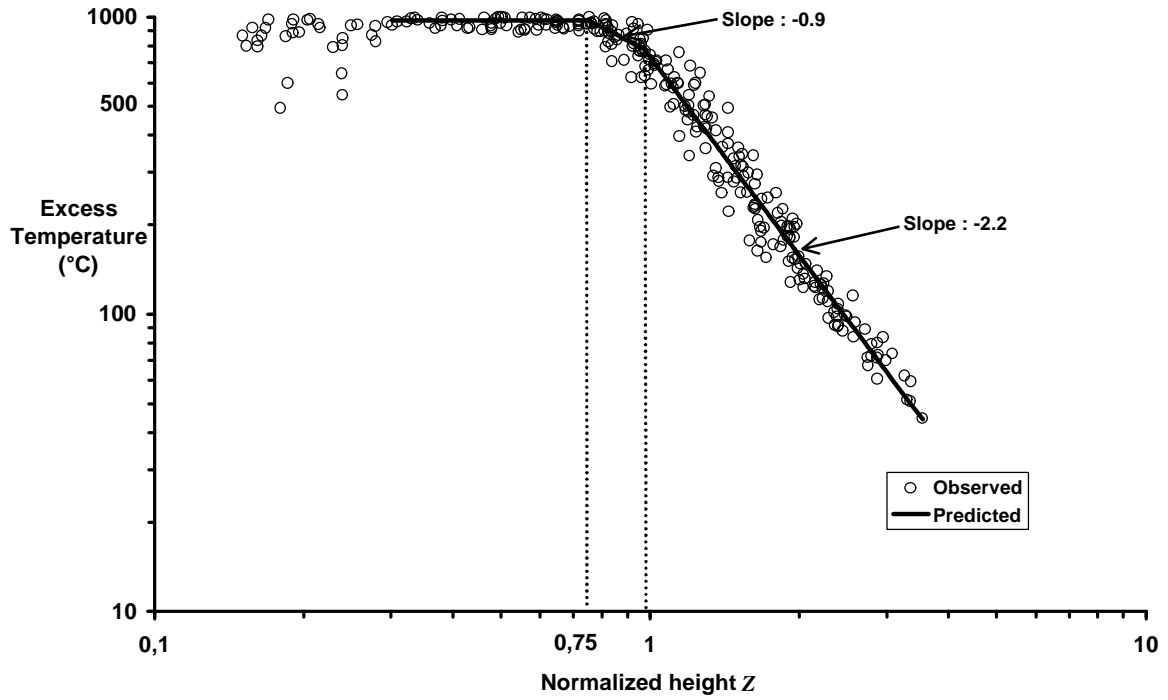


Figure 9. Vertical profile of maximum excess temperature.

3.4 Horizontal temperature profiles

As a first step, we analysed the horizontal profiles of maximum excess temperatures for each treatment (3 replications) and for each of the three horizontal levels located inside the flame or inside the plume (0.5, 1.5 and 2.5 m height). The maximum excess temperatures were normalized by the observed centreline temperature ($T_m - T_a$). It was found that a Gaussian function of the radius r described reasonably well the observed values. The analysis of the size parameter of the profiles showed that it is mainly influenced by the height of measurement z . In contrast to this, the burner diameter and the maximum heat release rate do not clearly affect the profile.

As a second step, we normalized the maximum excess temperatures by the predicted centerline temperatures at the corresponding height of measurement and we plotted the three horizontal profiles against a normalized radial position (ratio of the radius r to the height of measurement z), merging all the tests. Data are shown in Fig. 10. A Gaussian model describes reasonably well each of the profile :

$$\frac{T(z, r) - T_a}{T_m(z) - T_a} = k \exp\left(-a \left(\frac{r}{z}\right)^2\right) \quad (7)$$

The estimated parameters (mean and standard error) are :

- at $z=0.5$ m : $k=0.97$ (0.02), $a=17.8$ (0.7)
- at $z=1.5$ m : $k=0.97$ (0.02), $a=64.9$ (2.8)
- at $z=2.5$ m : $k=1.00$ (0.01), $a=63.9$ (3.0)

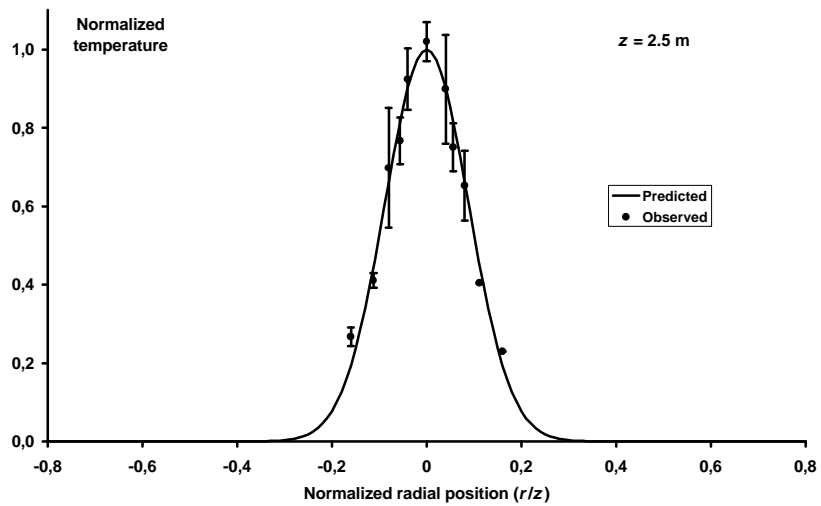
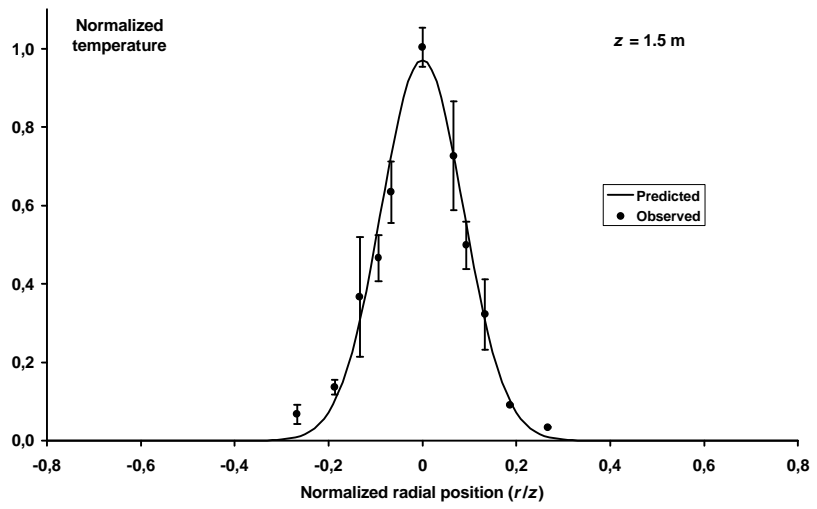
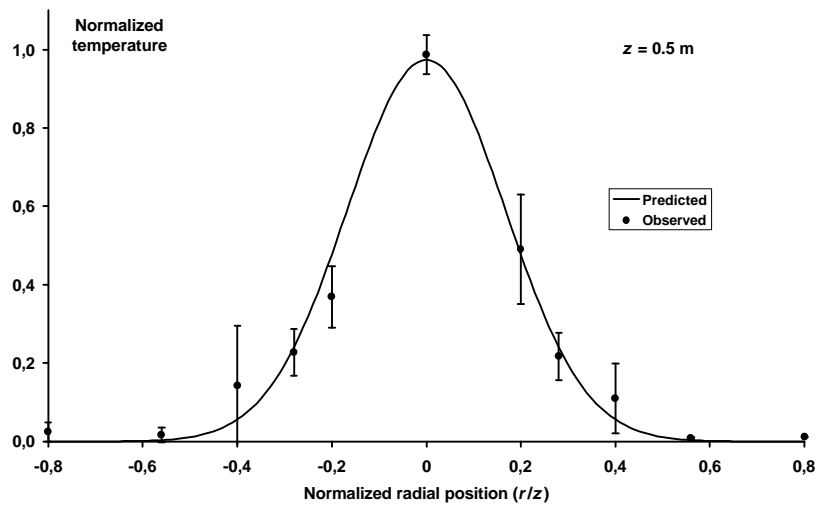


Figure 10. Horizontal profiles of normalized excess temperature.
(observed data : mean and standard deviation)

The predicted profiles respectively at 1.5 m height and 2.5 m height are not significantly different and data can be merged. In fact, these two heights of measurement are such that for each test, the normalised height Z is higher than 0.9. That means that all data of these profiles correspond to the upper part of the intermittent region of the flame or to the plume. In contrast, the profile obtained at 0.5 m height strongly differs from the two previous ones. For this height of measurement, the normalized height Z ranges between 0.3 and 0.6. That means that all data of this profile belong to the persistent flame.

Hence, we verify that a unique Gaussian horizontal profile of a half-width increasing linearly with the vertical position z , well describes the radial temperature in the plume region. This result is compatible with numerous studies of radial temperature profiles in thermal plumes and with the study of Gengembre & *al* (1984) on turbulent diffusion flames.

3.5 Thermal fluctuations and upward “gas” velocities

Cox (1977) describes and tests a method of measurement of gas velocity in fires based on the cross-correlation of thermal fluctuations. In fact, what is measured is the mean velocity of eddy structures. The principle of the method is to determine the transit time of a thermal fluctuation between two points of the flow where the temperature is measured. The three pairs of thermocouples of which the signal was recorded at a high frequency of 200 Hz were devoted to this analytical measurement of velocity. Fig. 11 shows a sample of the signals of a pair of thermocouples centred at 150 cm height. The high amplitude of the thermal fluctuations may be noticed. The time-lag between the two signals is visible (here 0.05 s).

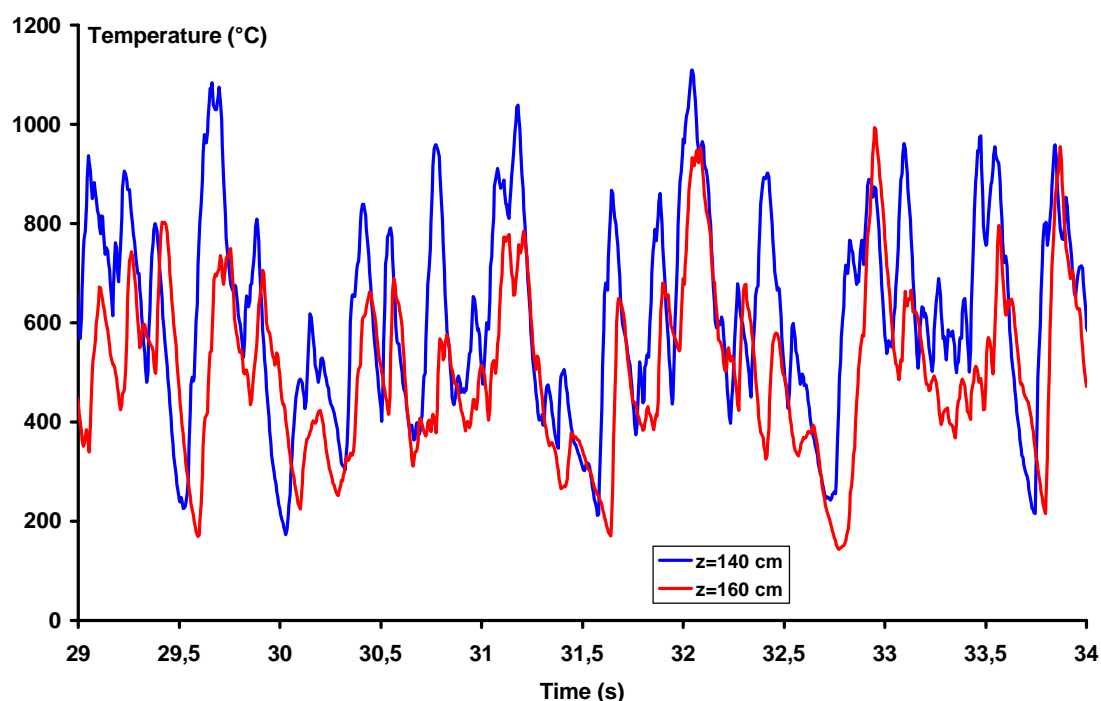


Figure 11. A sample of temperature signals recorded at 200 Hz (Fuel=PP, $D=0.4$ m, Plate=Yes).

The spectral analysis of the signals does not reveal any clear peak of frequency and shows that frequencies above 10 Hz do not contribute to the power spectrum. In fact, this is in accordance with the characteristic response time of the thermocouples (order of magnitude: 0.1 s), which corresponds to a cut-off frequency of 10 Hz.

The (normalized) cross-correlation function of two signals x and y measured in two points separated by a distance d is expressed as :

$$r_{xy}(d, \mathbf{t}) = \lim_{q \rightarrow \infty} \frac{1}{q} \int_0^q x(t - \mathbf{t}) y(t) dt \quad (8)$$

where x and y are normalized by their respective standard deviations and \mathbf{t} is the time shift. The auto-correlation function of the signal x is then $r_{xx}(0, \mathbf{t})$. The transit time \mathbf{t}_m corresponds to the maximum of the cross-correlation function.

According to Cox (1977), the method of cross-correlation is valid under the assumption of “frozen” turbulence. A strictly frozen turbulence would imply a cross-correlation peak equal to 1. Cox proposes that a measure of the departure from this assumption is obtained by a comparison of the space correlation $\rho_{xy}(d, 0)$ with the auto-correlation at a shifted time \mathbf{t}_m ($r_{xx}(0, \mathbf{t}_m)$). Hence, the shorter the distance between the thermocouples, the most valid is the assumption. But, as the distance between the thermocouples decreases, the transit time and the number of time-lags from zero will decrease. Then, the accuracy of the measurement decreases (for one time-lag, the relative uncertainty is 100 %). A compromise must be found between the two constraints.

As a first step, we tried a distance d of 10 cm. The order of magnitude of the maximum velocities was 4 m/s. Given the frequency of 200 Hz, this led to a relative uncertainty of +/-20 % on the estimated velocity. We then chose to increase the distance to 20 cm. In that case, the relative uncertainty of the velocity W is equal to 0.025 W , leading to +/- 10 % of uncertainty on a value of 4 m/s. The counterpart is that the assumption of “frozen” turbulence is less valid, but we have no means to measure its influence on the accuracy of the estimated velocity. We can indicate that for 90 % of the data, the difference between $r_{xy}(d, 0)$ and $\rho_{xx}(0, \mathbf{t}_m)$ is lower than 0.15 (median difference is 0.1), and the cross-correlation peak is higher than 0.7 (median is 0.77).

For each test, the cross-correlation and auto-correlation functions of each pair of thermocouples were estimated on a sample of 1000 points (5 s), centred on the time at which the maximum excess temperature was reached (maximum value of a moving average over a 5 s period, see 3.3). Fig. 12 provides an example of the estimation of the cross-correlation and the auto-correlation functions. The transit times and the upward velocities of “gases” (eddy structures) were deduced for each test. Table 2 provides the mean results for each treatment and each height of measurements.

Table2. Maximum values of flame height (H_{flmax}) and upward velocity of gases

Basket diameter(cm)	Fuel	Plate	H_{flmax} (m)	W (m/s) at 0.5 m height	W (m/s) at 1.5 m height	W (m/s) at 2.5 m height
40	PP	Yes	1.9	3.5	4.2	4.7
40	Exc	Yes	1.6	3.9	3.6	3.8
40	PP	No	2.0	4.3	4.1	4.4
40	Exc	No	1.9	3.9	4.2	4.3
28	PP	Yes	1.6	3.9	3.9	3.3
28	Exc	Yes	1.3	3.9	3.9	3.0
28	PP	No	1.7	3.8	3.8	3.7
28	Exc	No	1.4	3.9	3.4	3.3
20	PP	Yes	1.3	2.9	3.0	2.8
20	Exc	Yes	1.0	2.5	2.4	2.4
20	PP	No	1.3	3.4	3.0	2.8
20	Exc	No	1.1	3.1	2.5	2.7

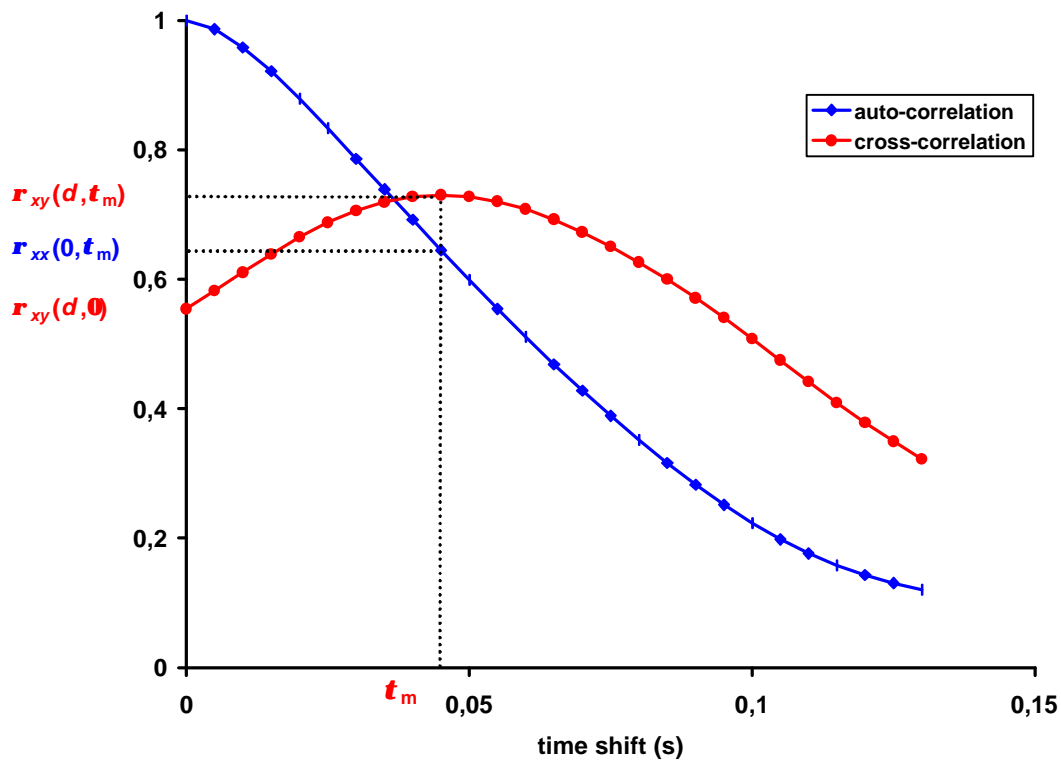


Figure 12. Estimated auto-correlation and cross-correlation functions for a pair of thermocouples located at $z=1.5$ m (Fuel=PP, $D=0.4$ m, Plate=Yes).

The only variable that significantly influences the velocity is the maximum heat release rate. For the upper height of measurement (1.5 and 2.5 m), the velocity is well correlated to the maximum heat release rate Q_{fmax} (Fig. 13). These points of measurement belong to the plume region ($Z_{fl} > 0.9$). According to McCaffrey (1979), the velocity in the plume region is correlated to a power of 1/3 of (Q_{fmax}/z) , but from the present data, we cannot see an effect of the vertical position z on the correlation.

For the first height of measurement (0.5 m), we do not find a clear correlation and it seems that the observed values belong to two distinct populations. For $Q_{fmax} < 75$, the velocity is equal to 3.0 m/s (*std dev.* 0.4). For $Q_{fmax} > 75$, the velocity is equal to 3.9 m/s (*std dev.* 0.5). These points of measurement belong to the persistent flame ($0.3 < Z_{fl} < 0.6$).

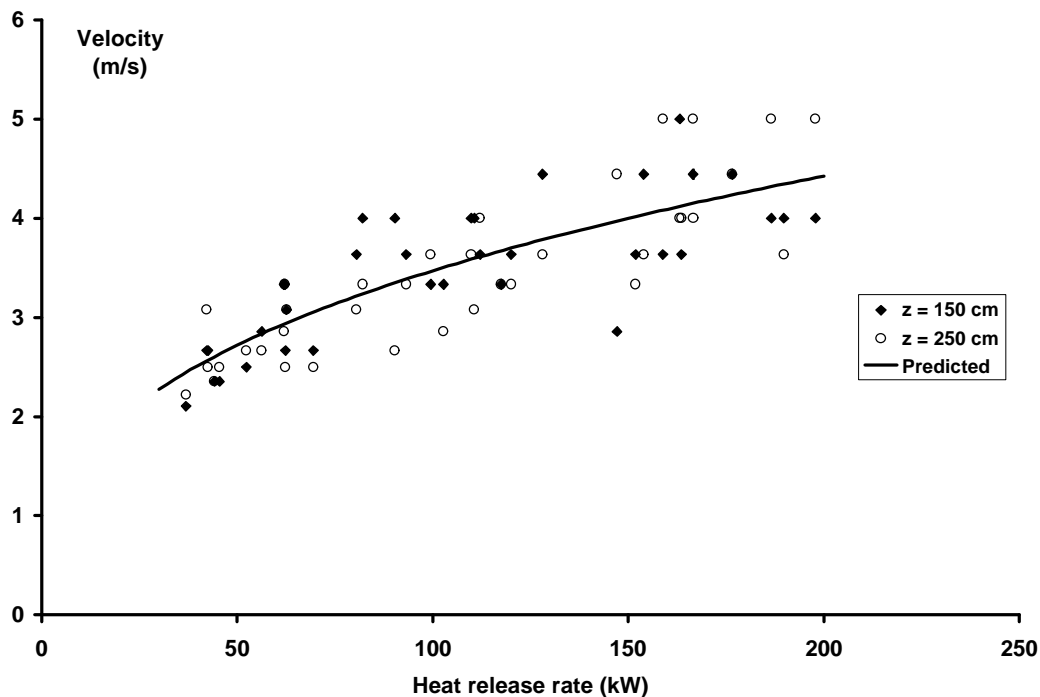


Figure 13. Upward velocity of eddy structures as a function of the heat release rate.

4 CONCLUSIONS

The objective of obtaining several regimes of combustion by combining the different treatments has been achieved. These regimes differ by the maximum heat release rate achieved during a test and the characteristic duration of the combustion. An essential difference with earlier studies of turbulent diffusion flames is that the present combustion regimes are strictly non-steady. Despite this difference, the usual scaling laws that enable to relate flame height, temperature profiles and upward gas velocity profiles to burner characteristics in the upper part of the flame and in the plume, hold for the maximum flame height, for the maximum temperatures and (less clearly) for the maximum upward velocities observed in the present study. However, we found that some of the parameters of the profiles numerically differ from earlier studies.

Hence, we will test if the complete physical model for fire behaviour that we are developing is able to render the main results of the study, namely the observed combustion regimes and the associated temperature profiles. The comparison will be complemented using a series of experiments we have performed on the same device, to test the ignition of a live branch of *Pinus halepensis* submitted to the hot gas flow stemming from the present burner.

The analytical method used in the present study to estimate the upward “gas” (eddy structures) velocity should be improved, probably by recording the temperature at higher frequencies than we did for this purpose (perhaps 1000 Hz instead of 200 Hz). We need to compare the results of this cheap and quite “simple” method, that measures a time-averaged eddy structure velocity and not the gas velocity, to an *a priori* very accurate method of measurement, namely the Laser Doppler Velocimetry. This work should be done on the same device in the next months and another method (Particle Image Velocimetry) will also be used to determine the field of velocities in a vertical plane. At present, we are dealing with thermal infrared measurements using a camera to evaluate some of the radiative properties of the flame. The objective is to make available a full set of measured physical properties that will be used to test the assumptions of the forest fire behaviour model and to improve it.

ACKNOWLEDGMENTS

We greatly acknowledge the French Ministry of Agriculture and Fishery (Direction de l'Espace Rural et de la Forêt) for its financial support (contract 6121-0598).

REFERENCES

- Cox, G. 1977. Gas velocity measurement in fires by the cross-correlation of random thermal fluctuations - a comparison with conventional techniques. *Combustion and Flame* **28**:155-163.
- Drysdale, D. 1998. Diffusion flames and fire plumes. *In An introduction to fire dynamics*, chapter 4. Ed. John Wiley & Son.
- Gengembre, E., Cambray, P., Karmed, D. & Bellet, J.C. 1984 Turbulent diffusion flames with large buoyancy effects. *Combustion, Science and Technology* **41**:55-67.
- Grishin A.M. 1997. *Mathematical modeling of forest fires and new methods of fighting them*. Publishing House of the Tomsk University, Tomsk Russia, F. Albini (Ed.).
- Larini, M., Giroud F., Porteie B. and Loraud J-C. 1998. A multiphase formulation for fire propagation in heterogeneous combustible media. *Int. J. Heat and Mass transfer* **41**(6-7):881-897.
- Linn, R.R. 1997. A transport model for prediction of wildfire behavior. PhD thesis, Los Alamos National Laboratory (LA-13334-T), University of California (UC-905), 195 p.
- Margerit J., Séro-Guillaume O. 2002. Modeling forest fires Part II: Reduction to two-dimensional models and simulation of propagation. *Int. J. Heat & Mass Transfer* **45**(8):1795-1722.
- Morvan, D. & Dupuy, J.L. 2001. Modeling of fire spread through a forest fuel bed using a multiphase formulation. *Combustion and Flame* **127**:1981-1994.
- Morvan, D., Tauleigne V. & Dupuy J-L 2002a. Wind effects on wildfire propagation through a Mediterranean shrub. *4th Int. Conf. Forest Fire Research*, Nov.2002, Coïmbra, Portugal.
- Morvan, D., Tauleigne V. & Dupuy J-L 2002b. Flame geometry and surface to crown fire transition during the propagation of a line fire through a Mediterranean shrub. *4th Int. Conf. Forest Fire Research*, Nov.2002, Coïmbra, Portugal.
- McCaffrey B.J. (1979) Purely buoyant diffusion flames : some experimental results. NBSIR79-1910, National Bureau of Standards, Washington, DC.
- Steward, F.R. 1970. Prediction of the height of turbulent diffusion flames. *Combustion, Science and Technology* **2**:203-212.
- Zukoski, E.E. 1995. Properties of fire plumes. *In Combustion fundamentals of fire*, chapter 3, ed. G.Cox. Academic Press, London.
- Zukoski, E.E, Kubota T. & Cetegen, B. 1981. Entrainment in fire plumes. *J. Fire Safety* **3**:107-121.